International Journal of Advanced Science and Technology
Vol.113 (2018), pp.93-102
http://dx.doi.org/10.14257/ijast.2018.113.10

Design and Analysis of a Meander Line Cornered Microstrip Patch Antenna with Square Slotted EBG Structure for ISM/WLAN Applications

Karteek Viswanadha* and Nallanthighal Srinivasa Raghava

[1]*Delhi Technological University*
[2]*Delhi Technological University*
[1]*karteekviswanath@gmail.com*, [2]*nsraghava@dce.ac.in*

Abstract

This paper presents the design and mathematical analysis of a fully efficient meander line edged microstrip patch antenna with square slotted Electromagnetic Bandgap (EBG) structure in Advance Design System-2016(ADS-2016). The proposed antenna is designed to have gain, directivity of 9.7dBi and cross polarization of -50dB at 17.92GHz which indeed makes it suitable for ISM/WLAN applications. Moreover, the simulation and mathematical results are in good agreement.

Keywords: *microstrip patch, gain, EBG, DGS, ADS, efficiency, bandwidth, slot, cross polarization*

1. Introduction

Design of wireless communication systems needs to be compatible and efficient. Along with many compatible radio amplifiers and mixers, planar antennas are also proposed which can be easily integrated with the transceiver. Many planar antennas like microstrip patch, Planar Inverted F-Antenna (PIFA) are used to achieve compactness and ease of integration. Microstrip patch antennas are widely used in many applications due to their ease of fabrication, compactness and planar nature [1]. Microstrip patch arrays are used in satellite transceivers due to the beamforming ability. A wide variety of patch antennas like the circular, bow-tie, and triangular are proposed to meet specifications such as wide bandwidth, high gain, polarization diversity and circular polarization. These antennas are highly directional and their gain varies from 4dBi to 7dBi depending on the shape of the patch. Gain and bandwidth are inversely proportional and there should be a trade-off between gain and bandwidth. These usually suffer from low bandwidth and high losses. Gain increases if the proper phase of excitation is provided to the patch array. Apart from patch arrays, slotted patches can be used in order to increase the gain at the cost of bandwidth [2].

Gain and directivity depend on the shape of the slot and the position of the slot. A multi slotted antenna is proposed to achieve gain of 9.4dBi and bandwidth of 0.58GHz in [3]. 3-dB bandwidth in azimuth and elevation planes is 60.88^o and 39^o respectively. The bandwidth and gain of a slotted patch antenna can also be increased by shorting the patch and the ground. This special feature is utilized in Planar Inverted F-Antenna (PIFA) [4]. A slot is made in the PIFA which makes the antenna to achieve a bandwidth of 1GHz at 0.89GHz and 1.93GHz respectively in [5]. Gain and bandwidth are varied by changing the length and width of shorting plate. The grooved slot antenna is proposed to achieve a bandwidth of 1.5GHz with a gain of 6dBi and reasonable Specific Absorption Rate (SAR) in [6]. The gain and bandwidth can be varied by varying the position of the shorted plate. This not only increases the above specifications but also compatibility. The electrical length of these antennas is reduced making them compatible at the expense of efficiency. These

Received (October 18, 2017), Review Result (January 10, 2018), Accepted (January 17, 2018)

ISSN: 2005-4238 IJAST

antennas have the capability to produce wide bandwidth in multiple bands. Circular shaped fractal PIFA antenna provides high efficiency and gain [7]. Reducing the area of the ground plane increases the efficiency and gain. The variation of position of shorting plate has no impact on gain and efficiency [8]. Varying the substrate features also affect the specifications of an antenna [9]. Multiple shorted pins PIFA is proposed where the side walls are covered with Perfect Electric Conductor (PEC) in [10]. Substrate inside the antenna box is tempered so as to improve the bandwidth and gain. The Antenna is tuned and bandwidth is enhanced using shorting straps [11]. The antenna consists of dual elements with dual shorting pins surmounted on a folded ground plane which acts as a perfect PEC case in [12]. Planar antennas are often prone to surface waves which severely affect the gain of these antennas.

In order to prevent the surface waves, the ground of planar antenna is drilled exactly below the antenna. This type of ground is named as Defective Ground Structure (DGS). DGS patch antennas reduce surface waves with the reduction in efficiency and increase in the side lobes [13]. Different shapes of DGS planar antennas are proposed in order to reduce the unwanted radiations. The variation in the size and positions of slots on the ground plane will shift the frequency of operation with the degradation in the performance of an antenna. Another method to reduce the surface waves is to place slots periodically on the ground plane except on the area below the planar antenna which is kept unetched. This type of structure is called electronic band gap structure [EBG] [14-17]. Planar antennas with EBG structures often provide high gain. Simple EBG Planar antennas can only possess high efficiency at L, S and C bands respectively [18-19]. At the upper band of extremely high frequencies, EBG planar antennas provide high directivity with low efficiency and therefore the gain of these antennas decreases at the Ku, K, Ka bands etc. Usually antennas become electrically small when the operating frequency shifts towards higher bands. Ohmic losses also increase at higher bands and thereby decreasing the efficiency of the antenna.

Mathematical analysis is often carried out before antenna can be designed, simulated and realised practically. Antennas are analysed using many mathematical methods [12] like Green's function, Finite Difference Time Domain Method (FDTD), full wave analysis, Finite Element Method (FEM), Method of Moments (MoM) *etc*. In [13-14], the radiating structures are analysed mathematically using Green's functions. Dyadic Green's functions are derived for a slot using Helmholtz's equation as a base. Dyadic Green's functions are used for the computation of electric and magnetic fields.

This paper presents the designs and analysis of meander line cornered microstrip patch antenna with square slotted EBG at 17.92GHz with improved gain, directivity and efficiency.

2. Design of Proposed Antenna

Meander antenna is electrically small antenna. A basic meander line consists of a set of horizontal and vertical lines. Efficiency of a meander line antenna depends on the number of turns of a meander. Moreover, the resonant frequency of the proposed antenna depends on the spacing between the meander lines. Figure.1 shows the layout in Advanced Design System-2016 of the proposed antenna with length equal to 7.7mm and width equal to 11.1mm calculated from the below design equations. Antenna is mounted on the EBG of length (L) equal to 19.25mm and width (W) equal to 27.75mm. EBG slots of square type with side (a) of 1mm. Spacing (s) between two EBG slots is chosen to be 0.2mm. Meander lines are placed at the corners of the patch. Width (w_1) and length (a_o) of the meander lines are 0.762mm and 1.24mm respectively.

RT-Rogers/duroid 5880 ($\varepsilon_r = 2.2$) is used as a substrate which is sandwiched between EBG structure and the proposed patch antenna with the height of 2.54mm respectively. Moreover, a notch is made on the non-radiating side of the patch with the width and length (t) of 0.762mm and 1.52mm respectively. Inset feed is used to excite the antenna with the feed line having length (l_o) and width (w_o) of 2.24 mm and 1.2 mm respectively. Inset into feed is inserted to chosen to have depth and length of 0.12mm and 0.23mm respectively.

The design equations of inset fed microstrip patch antenna are:

$$\frac{\Delta L}{h} = 0.412\frac{(\varepsilon_{eff}+0.3)(\frac{W_p}{h}+0.264)}{(\varepsilon_{eff}-0.258)(\frac{W_p}{h}+0.8)} \quad (1)$$

$$h \approx 0.06\frac{\lambda_{air}}{\sqrt{\varepsilon_r}} \quad (2)$$

$$W_p=\frac{c}{f_r}\sqrt{\frac{2}{\varepsilon_r+1}} \quad (3)$$

$$\varepsilon_{eff} = \frac{\varepsilon_r+1}{2} + \frac{\varepsilon_r-1}{2}\frac{1}{\sqrt{1+12h/W}} \quad (4)$$

$$L_p=\frac{c}{2f_r}-2\Delta L \quad (5)$$

‘h’ is the height of the substrate
‘W_p’ is the width of the patch
‘ε_{eff}’ is effective dielectric constant
‘L_p’ is the length of the patch
‘ΔL’ is the normalized extension length
‘f_r’ is the resonant frequency
‘c’ is the velocity of light

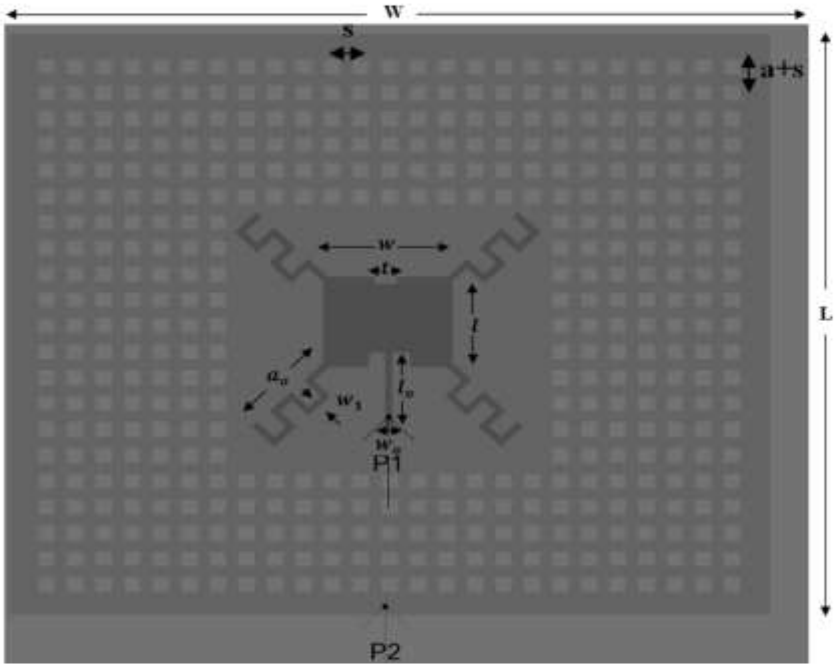

Figure 1. Layout of the Proposed Antenna

Figure 2 (a) & 2(b) shows the 3-D model and top view of the proposed patch antenna. The whole structure is designed on an infinite ground assumed to be a perfect electric conductor.

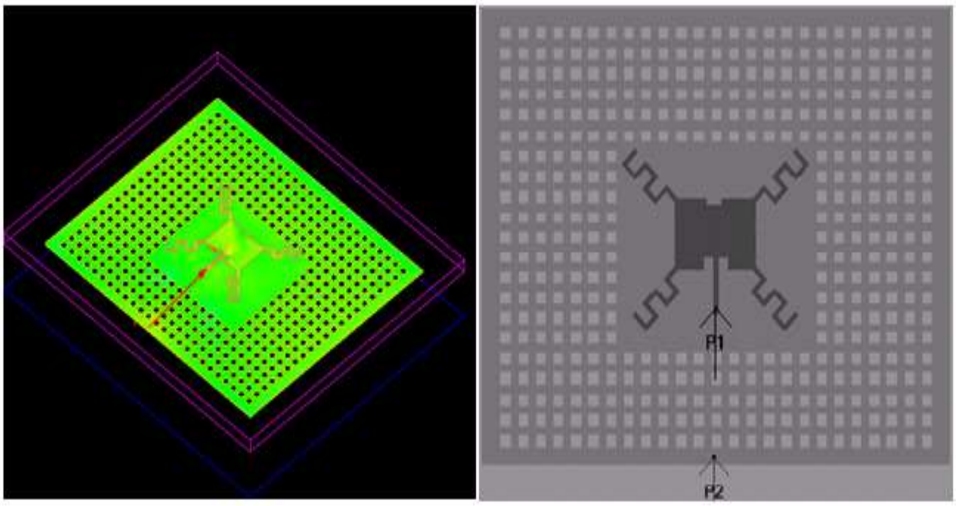

Figure 2(a). 3-D Model of the Proposed Patch Antenna
Figure 2(b). Top View of the Proposed Patch Antenna

EBG structures are periodical slots composed of metallic elements. The purpose of these structures is to create the forbidden band of frequencies in which surface waves cannot propagate. Microstrip patch antennas suffer from surface waves as the excited signals are reflected by the patch and get trapped inside the substrate. These waves reduce antenna efficiency and gain, limit bandwidth, increase radiation in the non-radiating edges of the patch, increase cross polarization levels, and limit the bandwidth of microstrip antennas. When the antenna operates in the forbidden gap of frequencies, gain, bandwidth and radiation efficiency decreases. An antenna that is placed on a low-permittivity dielectric substrate may couple power into substrate modes. The band gap formation in EBG is due to the interplay between macroscopic and microscopic resonances of a periodic structure [24, 25]. The periodicity governs the macroscopic resonance or the Bragg resonance, the lattice resonance, whereas the microscopic resonance is due to the element characteristics, and it is called the Mie resonance [23].

When the two resonances coincide, the structure possesses a band gap having maximum width. The electromagnetic nature of a surface is predictable from the reflection phase characteristics, such that a 180° reflection phase implies a perfect electric conductor (PEC) surface and a 0° reflection phase resembles a perfect magnetic conductor (PMC) surface. If a plane wave is normally impinged upon a PEC, the total tangential field must be zero in order to satisfy the boundary condition. Thus, the reflected field and the incident field should have the opposite signs, resulting in a reflection coefficient of −1. The reflection phase is 180° for the PEC case. Similarly, for a PMC, the reflected field and the incident field should have the opposite signs whereas the reflected field and the incident field have the same signs. As a result, the reflection coefficient is equal to +1, and the corresponding reflection phase is 0° for PMC case [26]. Depending on the structural characteristics and polarization of the wave, one of the stop band resonance mechanisms can dominate over the other [4].

At the stop band, the structure will reflect back all electromagnetic waves, whilst at other frequencies, it will act as a transparent medium. EBG structure consists of three portions: a metallic ground, a substrate on which the periodic metallic patches are surmounted. The proposed EBG structure is designed to have side ‘a’, spacing between the slots ‘s’, substrate height ‘h’ and dielectric constant 'ε_r'. When the periodicity (a + s) is small compared to the operating wavelength, the operation mechanism of the proposed EBG structure can be explained using an effective medium model with lumped LC elements. The capacitor results from the gap between the patches and the inductor results from the current along adjacent patches. Capacitor results due to the air gap of the slot and inductor results due to the current flow in the adjacent slots.

Impedance and resonant frequency of the parallel LC circuit are calculated given by:

$$Z = \frac{j\omega L}{(1-\omega^2 LC)} \tag{6}$$

$$\omega_o = \frac{1}{\sqrt{LC}} \tag{7}$$

$$C = \frac{a\varepsilon_o(1+\varepsilon_r)}{[\pi \cosh^{-1}\left[\frac{s+a}{a}\right]]} \tag{8}$$

$$L = \mu_o h \tag{9}$$

3. Cavity Model of the Proposed Antenna

The whole patch is analyzed using cavity model by considering later as rectangular resonator and Figure.3 shows the proposed patch with a single meandered line. The metallic patch forms a resonant cavity [20]. Top, bottom, and sides of the cavity are formed by the patch, ground and edges of the patch respectively. The edges of the patch act approximately as an open-circuit boundary. The energization of the patch will establish a charge distribution on the upper and lower surfaces of the patch as well as on the surface of the ground plane [21-22]. Hence, the patch acts approximately as a cavity with tangential electric and magnetic fields absent on the top, bottom, and sides of the cavity. 'P' is the observation point from where the far fields are observed. Radiated fields of patch and the meander line are superimposed at 'P'. Electric field is directed towards z-axis *i.e.*, $\vec{E} = \bar{z}E_z(x, y)$. The z-component of electric field satisfies Helmholtz's equation:

$$\frac{\partial^2 E_Z}{\partial x^2} + \frac{\partial^2 E_Z}{\partial y^2} + {k_c}^2 E_Z = 0$$

Using the boundary conditions, currents at the edges of the patch are zero and voltages on the patch are zero.

Therefore, $E_Z = E_o \cos\left(\frac{m\pi x}{l+a_o}\right) \cos\left(\frac{n\pi y}{w+2w'}\right)$

Where l, a_o, w and w' are the lengths and widths of patch and meander lines as shown in Figure 1.

Patch is in the X-Y plane, the radius vector $\acute{r} = x\bar{a}_x + y\bar{a}_y$ and $\bar{n}$ is the unit vector the XY plane. $\bar{n} = \bar{a}_z$

Converting radius vector into spherical coordinates,
$r = \sin\theta\cos\phi\bar{a}_x + \cos\theta\cos\phi\bar{a}_y + \cos\theta\bar{a}_z$ and $dS = dxdy$

$$D_\theta(\theta, \phi) = E_o \frac{wl}{2} \text{sinc}((l + a_o)\sin\theta\cos\phi)\text{sinc}((w + w')\cos\phi)\bar{a}_\theta \tag{10}$$

$$D_\phi(\theta, \phi) = E_o \frac{wl}{2} \text{sinc}((l + a_o)\sin\theta\cos\phi)\text{sinc}((w + w')\sin\theta\cos\phi)\bar{a}_\phi \tag{11}$$

Magnetic vector potential is given by
$A = G\,(r, r_o)[-D_x(\theta, \phi)\bar{a}_z + D_z(\theta, \phi)\bar{a}_x]$, where $G\,(r, r_o)$ is Green's function given by $\frac{e^{-j\beta r}}{4\pi\varepsilon r}$

$$E_\theta = E_o \frac{j\omega w l e^{-j\beta r}}{4\pi\mathcal{E}r} \text{sinc}((l + a_o)\sin\theta\cos\phi)\text{sinc}((w + w')\cos\phi) \quad (12)$$

$$E_\phi = E_o \frac{j\omega w l e^{-j\beta r}}{4\pi\mathcal{E}r} \text{sinc}((l + a_o)\sin\theta\cos\phi)\text{sinc}((w + w')\cos\theta\sin\phi) \quad (13)$$

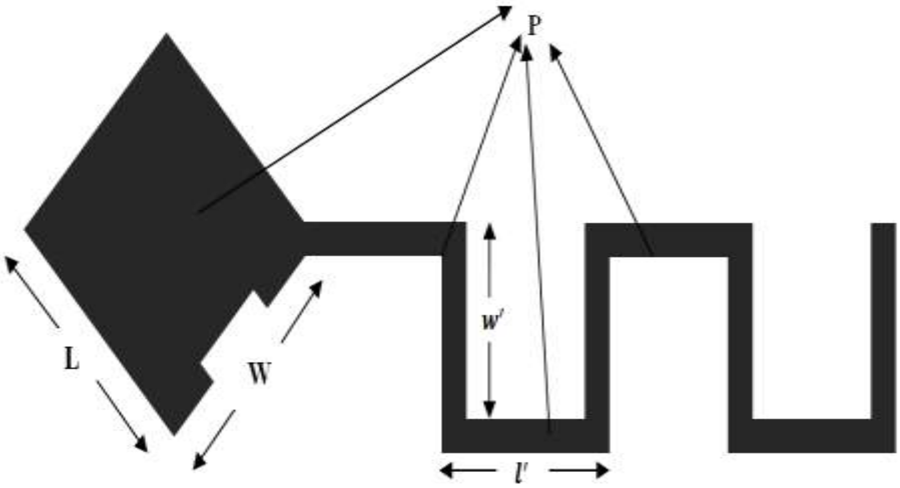

Figure 3. Meandered Line Microstrip Patch Antenna

4. Results and Discussions

Figure 4 shows the magnitude plot of reflection co-efficient of the proposed antenna. A reflection co-efficient of -10.166dB is obtained at 17.92GHz.

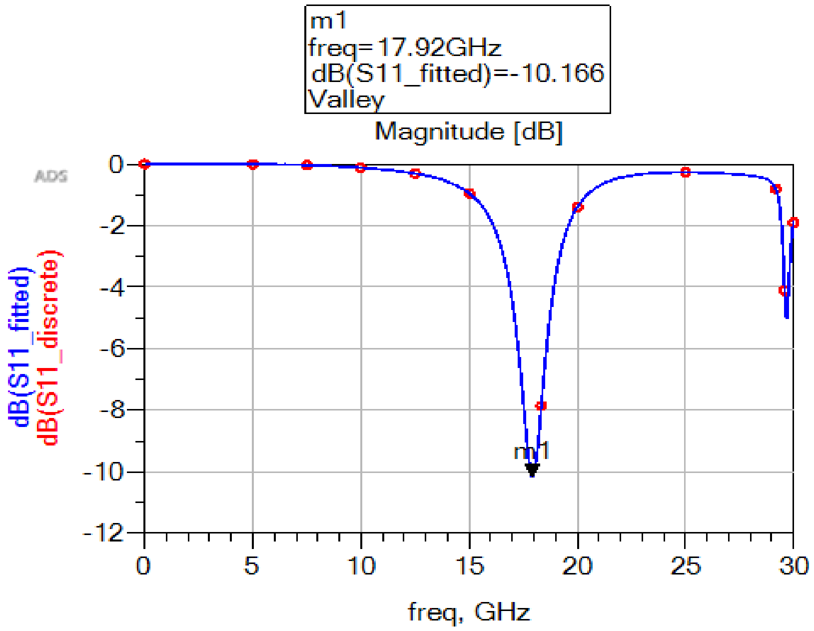

Figure 4. Magnitude and Phase Plot of Reflection Co-Efficient

Increasing number of slots on the ground plane has increased reflection losses to -8.2dB at 18 GHz. At the same time decreasing the number slots has degraded gain as well as bandwidth. Therefore, iterations are carried in order to obtain good agreement between number of slots, gain and bandwidth. Moreover, the operating frequency, gain and bandwidth of overall structure depend on the position of the patch on the EBG structure.

The proposed choice of slot dimensions highly reduced surface waves. Figure 5 shows the 3-D plot of the radiation pattern of the proposed antenna and the values of parameters related to the radiation pattern.

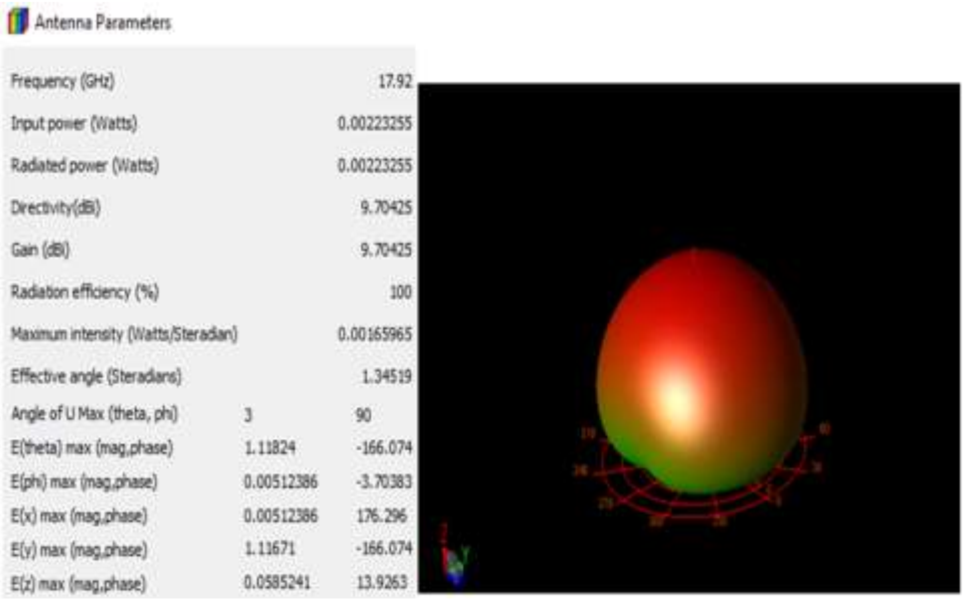

Figure 5. 3-D Plot of Radiation Pattern

Figure.6 shows the evaluated and simulated results of E fields in E and H-planes from the equations (12) & (13) respectively. A change of 0.01mm in the side of the square slot shifts the operating frequency by 3GHz with the degradation of both gain and bandwidth. Moreover, radiation pattern gets highly affected by the change in the width of the square slot. Hence, a trade-off has been maintained to between dimensions of the slot, gain, bandwidth and reasonable radiation pattern

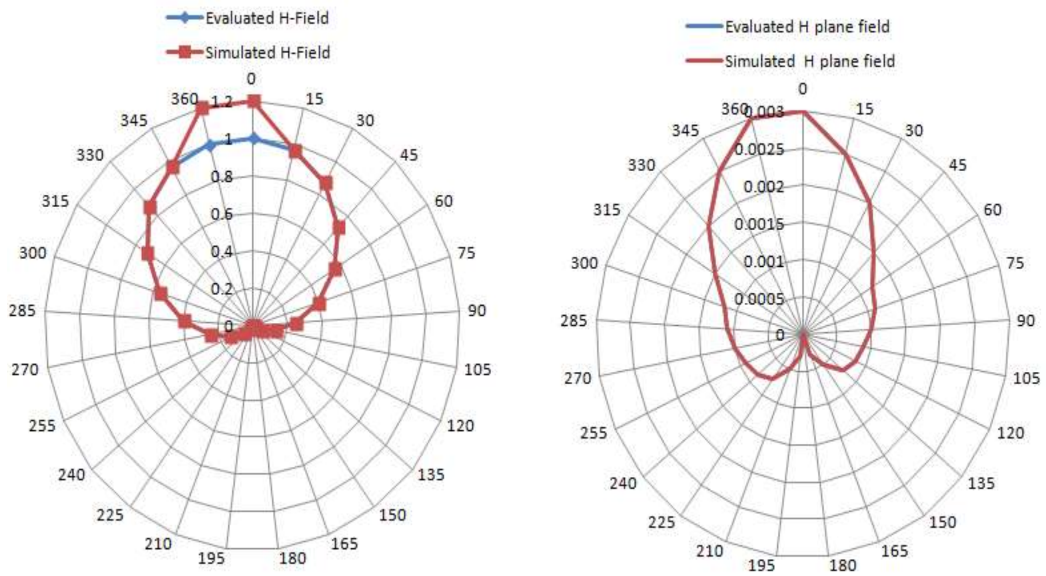

Figure 6. Evaluated and Simulated Electric Fields

Figure 7 shows the consolidated 2-D plot of gain, directivity, co-polarization, cross polarization *etc*. The side lobes are totally suppressed and the directivity is enhanced. The efficiency of the antenna varies with the dimensions of meander lines.

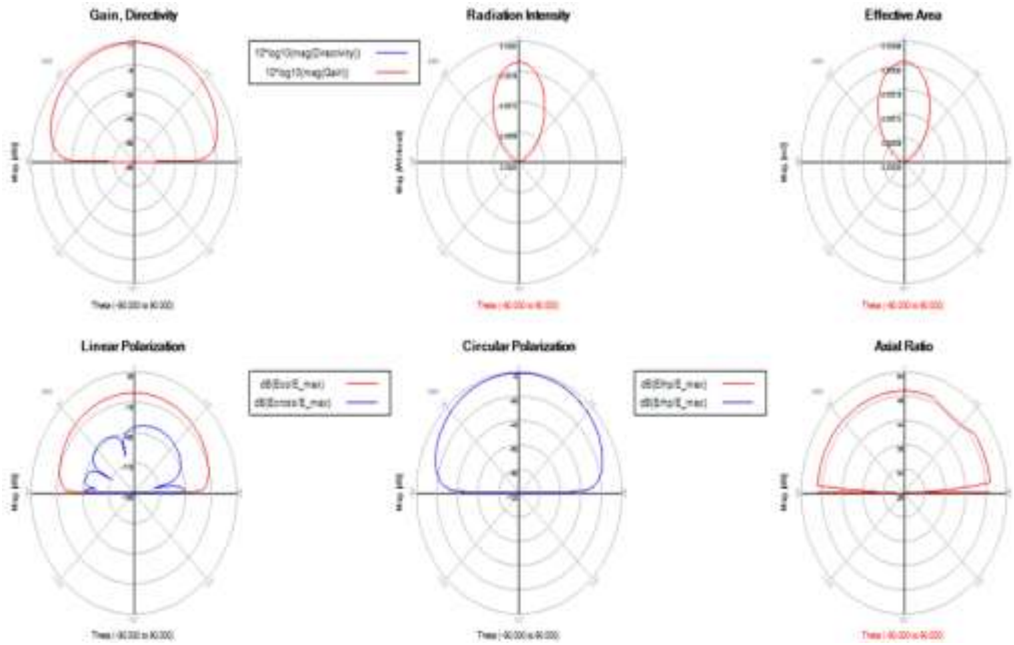

Figure 7. Consolidated 2-D Plot of all the Parameters of Antenna

Efficiency of the antenna varies with the spacing between the meander lines. A small change in the variation in the spacing increases efficiency by significant change with the disturbance in the radiation pattern. A reasonable trade-off is maintained between length, width, and spacing between the meander lines so that the antenna parameters are not affected. A small change in any of these parameters will affect gain and/or bandwidth and/or efficiency and/or radiation pattern. Table.1 shows the various parameters of the proposed antenna is presented at the resonant frequency of 17.92 GHz. The polarization of antenna depends on the spacing between the meander lines. The cross-polarization increases if the meander lines are closer to each other. Hence, proper spacing has been chosen in order to cancel out the magnetic fields radiated by the meander lines. The directivity of the proposed antenna depends on the length of the vertical line of the meander. Proper lengths of vertical lines are chosen in order to obtain high directivity. The use of too many turns in the meander lines may degrade gain, bandwidth and operating frequency. The width and length of the meander lines decide the input impedance and operating frequency respectively. A change of 0.01mm in the widths of the arms of the swastika shifts the operating frequency by 3GHz with the degradation of both gain and bandwidth. Moreover, radiation pattern gets highly affected by the change in the width of the meander lines. Hence, a trade-off has been maintained to between width of the lines, gain, bandwidth and reasonable radiation pattern.

Table 1. Performance Parameters of the Proposed Antenna

Gain (dB) (Fig.5)	Directivity (dB) (Fig.5)	Reflection Coefficient (dB) (Fig.4)	Cross Polarization (dB) (Fig.7)	Efficiency (%) (Fig.5)	Bandwidth (MHz) (Fig.4)
9.7	9.7	-10.166	-50	100	100

5. Conclusion

A high gain meander line cornered patch antenna is presented in this paper. The same gain can be achieved using 2-element microstrip patch array at the expense of compactness. The meander edged patch antenna provides high gain and efficiency with compactness. The above results of the proposed antenna make it suitable for the high data communications and especially for the ISM/WLAN applications. The used of unequal length and width in the meander lines also improves reflection coefficient. Moreover, the bandwidth can also be enhanced by using Split Ring Resonator (SRR) or Complementary Split Ring Resonator (CSRR) metamaterials. These materials should be embedded inside the substrate in order to achieve the best performance of the proposed antenna.

References

[1] A. Majumder, "Rectangular Microstrip Patch Antenna Using Coaxial Probe Feeding Technique to Operate in S-Band", International Journal of Engineering Trends and Technology (IJETT), vol. 4, no. 4, **(2013)**, pp. 1206-1210.

[2] Y. Liu, L.-M. Si, M. Wei, P. Yan, P. Yang, H. Lu, C. Zheng, Y. Yuan, J. Mou, X. Lv and H. Sun, "Some Recent Developments of microstrip patch antenna", International Journal of Antennas and Propagation, **(2012),** pp. 1-10.

[3] S. Gupta and E. Johari, "Dual Band Slotted Microstrip Patch Antenna for Wireless Applications", Journal of Physical Sciences, Engineering and Technology, **(2015)**, pp. 51-56.

[4] N. Kumar, A. Thakur and S. Jitender, "Study of Planar Inverted-F Antenna (PIFA) for Mobile Devices", International Journal of Electronics & Communication Technology, vol. 4, no. 3, **(2013)**, pp. 83-85.

[5] N. Firoozy and M. Shirazi, "Planar Inverted-F Antenna (PIFA) Design Dissection for Cellular Communication Application", Journal of Electromagnetic Analysis and Applications, **(2011)**, pp. 406-411.

[6] S. Saini, S. Singh and N. Kumar, "A Review of Various Planar Inverted Fantenna (PIFA) Structures for Wireless Applications", International Journal of Electrical & Electronics Engg, **(2015)**, pp. 63-65.

[7] W. He, Jian and K. Seng Chung, "Design Considerations of Planar Inverted-F Antenna (PIFA) On A Finite Ground Plane", International Symposium on Multi-Dimensional Mobile communications, **(2004)**, pp. 655-659.

[8] T.-H. Son and J.-H. Lee, "Inverted Π Feeding PIFA for Gain Improvement for the Mobile Phone", The Journal of Korean Institute of Electromagnetic Engineering and Science, **(2007)**, pp. 1337-1344.

[9] G. Kristensson, P. Waller and A. Derneryd, "Radiation Efficiency and Surface Waves for Patch Antennas On Inhomogeneous Substrates", IEEE Proceedings - Microwaves, Antennas and Propagation, **(2003)**, pp. 474-477.

[10] M. Sajjad Ahmad and C. Young Kim, "Dual-Element PIFA Design with Dual Shorting Pins for Multiband Communication Devices", International Journal of Antennas and Propagation**, (2015)**, pp. 1-8.

[11] H. T. Chattha, Y. Huang and Y. Lu, "PIFA Bandwidth Enhancement by Changing the Widths of Feed and Shorting Plates", IEEE Antennas and Wireless Propagation Letters, vol. 8, **(2009)**, pp. 637-640.

[12] M. Sajjad Ahmad and C. Young Kim, "Dual-Element PIFA Design with Dual Shorting Pins for Multiband Communication Devices", International Journal of Antennas and Propagation, **(2015)**, pp.1-8.

[13] M. Sontakke, V. Savairam, S. Masram and P. P. Gundewar, "Microstrip Patch Antenna with DGS for Bluetooth Application", International Journal of Engineering Research, vol. 6, no. 3, **(2017)**, pp. 524-527.

[14] N. S. Raghava and A. De, "A broadband compact microstrip antenna with EBG structure", Kalpana Chawla Space Technology Cell, IIT, Kharagpur, India, **(2008)**.

[15] K. Shivam Guatam and N. S. Raghava, "Design and Analysis of Uniplanar Compact Electromagnetic Bandgap Structures", Progress in Electromagnetics Research Symposium, Prague, Czech Republic, **(2015)**, pp. 2092-2094.

[16] N. S. Raghava and A. De, "Dual frequency Square Slot Rectangular Microstrip antenna with electronic band gap ground", 8th International Conference on Microwaves, Antenna Propagation and Remote Sensing (ICMARS-2012), Jodhpur, India, **(2012)**.

[17] D. Singh, N. S. Raghava, A. Biswas and A. De, "Dual frequency rectangular notch square microstrip antenna with EBG", International Symposium on Microwaves, Banglore, India, **(2008)**.

[18] A. Choudhary, N. S. Raghava, A. Biswas and A. De, "A Highly Efficient Rectangular Microstrip Antenna with Hexagonal Holes as an Electromagnetic Bandgap Structure in the Ground Plane", Recent Advances in Microwave Theory and Applications, India, **(2008),** pp. 152-153

[19] A. Choudhary, N. S. Raghava and A. De, "A High Gain Rectangular Patch Radiator with Square Holes in the Ground Plane", European Electromagnetic Symposium, Switzerland, **(2008)**.

[20] D. D. Sandhu, O. G. Avadanei, A. Ioachim and D. Ionesi, "Contribution to the cavity model for analysis of microstrip patch antennas", Journal of Optoelectronics and Advanced Materials, vol. 8, no. 1, **(2006)**, pp. 339-344.

[21] Y.-B. Gan, C.-P. Chua and L.-W. Li, “An enhanced Cavity model for Microstrip Patch Antennas”, Microwave and Optical Technology Letters, vol. 40, no. 6, **(2004)**, pp. 520-523.
[22] M. Mahajan, S. K. Khah and T. Chakravarty, “Extended Cavity Model Analysis of Stacked Circular Disc”, Progress in Electromagnetics Research, vol. 65, **(2007)**, pp. 287-308.
[23] S. F. Mahmoud, “A new miniaturized annular ring patch resonator partially loaded by a metamaterial ring with negative permeability and permittivity”, IEEE Antennas and Wireless Propagation Letters, vol. 3, no. 1, **(2004)**, pp. 19-22.
[24] A. Alù, M. G. Silveirinha, A. Salandrino and N. Engheta, “Epsilon-near-zero metamaterials and electromagnetic sources: tailoring the radiation phase pattern”, Physical Review B, vol. 75, no. 15, Article ID 155410, 13 pages, **(2007)**.
[25] M. S. Alam, M. T. Islam and N. Misran, “Inverse triangular shape CPW-fed antenna loaded with EBG reflector”, Electronics Letters, vol. 49, no. 2, **(2013)**, pp. 86-88.
[26] Md. S. Alam, N. Misran, B. Yatim and M. Tariqul Islam, “Development of Electromagnetic Band Gap Structures in the Perspective of Microstrip Antenna Design”, International Journal of Antennas and Propagation, vol. 2013, **(2013)**, pp. 1-22.

Authors

Mr. Karteek Viswanadha, he received B.Tech in electronics and communication from G.V.P College of Engineering (Autonomous), Visakhapatnam in 2007 and master in communication systems from Birla Institute of Technology and Sciences, Pilani (B.I.T.S, Pilani) in 2009. He is presently pursuing Ph.D in the area of millimeter wave devices and antennas from Delhi Technological University (Formerly Delhi College of Engineering), New Delhi.

Mr. Nallanthighal Srinivasa Raghava, he is working as Professor in Electronics and Communication Engineering Department at Delhi Technological University (Formerly Delhi College of Engineering), New Delhi. His area of specialization is Antenna and Propagation, Microwave Engineering, Digital Communication, Wireless Communication, Cloud Computing, Information Security.

